Axial-Flux PM BLDC Machines with Concentrated Windings: Double-Layer, Single-Layer, and Single-Layer with Unequal Tooth

Min Gu, Zijian Xi

Axial-Flux PM BLDC Machines with Concentrated Windings: Double-Layer, Single-Layer, and Single-Layer with Unequal Tooth

Min Gu
Department of Electrical Engineering
Guangdong University of Foreign Studies
Guangzhou, China
min.gu1980@gmail.com

Zijian Xi
Departament of Electrical Engineering
Guangdong University of Foreign Studies
Guangzhou, China
z.xi_uni@yahoo.com

***Abstract*—This paper investigates axial-flux permanent-magnet brushless-dc (PM BLDC) machines with concentrated windings and different layer numbers. In order to analyze the influence of layer numbers and unequal tooth on machine performance, three axial-flux PM BLDC machines are considered, and compared with respect to phase back-EMF, winding inductance, cogging torque, and electromagnetic torque. Three-dimensional (3-D) finite-element analysis is used to study the machines precisely.**

Keywords— axial-flux permanent-magnet, unequal tooth, single-layer, BLDC, 3-D finite-element analysis

I. INTRODUCTION

In term of flux flow, electrical machines can be classified either as radial-flux machines or axial-flux machines. In radial-flux machines, the magnetic flux moves along the radius in the air-gap, while in axial-flux machines the magnetic flux moves along the axial axis in the air-gap. An axial-flux PM machine provides higher power density compared with a radial-flux PM machine, and is a very attractive choice especially when an electrical machine has to be directly mounted into a mechanical machine [1-3].

Recently, technology of axial-flux PM machine with concentrated winding is emerging due to their high torque-density, high efficiency, compact construction, high filling factor especially with segmented stators, and good heat removal configuration [1-5]. Also, PM BLDC machines are known for their high efficiency and high torque-density [3,6]. So, axial-flux PM BLDC machines with concentrated windings are excellent choices to be used in applications with restrict space as in direct-driven applications, such as electric vehicles [7-9].

In PM machines with concentrated windings, stator coils may be wound either on all teeth (double-layer windings) or only on alternate teeth (single-layer windings). When single-layer winding is used, number of coils is halved. So the number of turns per coil must be doubled to have the same number of total series turns per phase as well as the same winding current density. In the case of using *similar* slot number and pole number, higher winding factor will be achieved which results in higher torque. Also, similar slot number and pole number results in low cogging torque. When an axial-flux PMBLDC motor with high torque density is considered for applications with limited space, similar slot number and pole number is an attractive choice. This paper investigates influence of unequal tooth widths and different layer numbers for axial-flux PM BLDC machines with similar slot number and pole number. Hence, the performance of three 3.4 kW 12-slot/10-pole axial-flux PM BLDC machines with double-layer windings, single-layer windings, and single-layer windings with unequal tooth widths are analyzed. In this research cogging torque, back-EMF, winding inductance, and output torque are obtained for the three axial-flux PM BLDC machines by 3-D finite element method.

II. MACHINE DESIGN CONSIDERATION

Axial-flux PM machines have different topologies. A high efficient axial-flux PM machine with segmented stator designed for electric vehicles [10-14] is chosen for this study. This novel axial-flux machine topology has gained attention and been used in different researches, particularly as in-wheel electric motors in lightweight urban electric vehicles. The machine has a single stator that is sandwiched between two surface-mounted PM rotor discs. The stator segments are stacked together as an integrated stator by high strength resin holders. Also parallel slot-opening is employed.

To analyze the influence of layer numbers and tooth widths, all the considered machines have the same dimensions, and the same pole and slot combination. In machines with low pole numbers, such as a 4 pole machine, rotor back-iron length must be increased to avoid saturation and may exceed the limited axial length of the motor for different applications with limited space. In machines with high pole numbers, such as an 18 pole machine, inter-pole leakage flux increases and will cause the air-gap flux-density distribution and back-EMF waveform to be more sinusoidal which is not desired for BLDC operation. High pole numbers also cause high manufacturing cost. After careful consideration and analyzing different pole numbers by 3-D finite-element method, 10 pole machines are chosen for investigation. Number of slots is set to 12 as in machines with similar slot number and pole number, higher winding factor

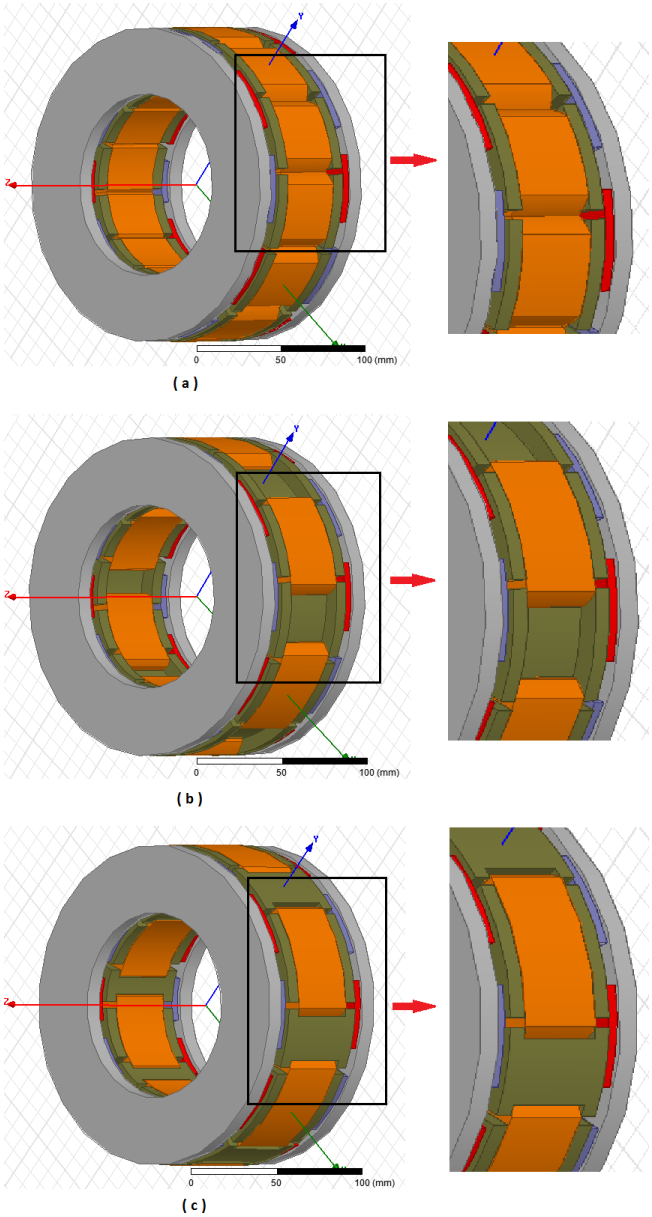

Figure 1. Winding configurations for 12-slot/10-pole machines (a) double-layer windings (b) single-layer windings(c) single-layer windings with unequal tooth widths

and hence higher output torque is achieved. Also, similar slot number and pole number results in low cogging torque due to high LCM (least common multiple) of pole number and slot number. Therefore the research is carried out for a 12-slot/10-pole axial-flux PM motor with double-layer windings (motor A), a 12-slot/10-pole axial-flux PM motor with single-layer windings (motor B), and a 12-slot/10-pole axial-flux PM motor with single-layer windings with unequal tooth widths (motor C). Figure 1 (a)-(c) shows motor A, motor B, and motor C; respectively. It is seen in Figure 1 (c) that the coils are wound on alternate teeth which are wider than unwound teeth. The widths of the wound teeth are set equal to the pole pitch so that pitch factor of 1 would be achieved.

TABLE I. MOTOR PARAMETERS

Motor type	A	B	C
No-load Voltage , V	50	50	50
Rated phase current, A	34	34	34
Rated rotational speed, rpm	1200	1200	1200
Stator outer radius, mm	95	95	95
Stator inner radius, mm	55	55	55
Slot-opening, mm	4	4	4
Tooth width at average radius, mm	35.27	35.27	43.12 27.41
pole-arc to pole-pitch ratio	0.7	0.7	0.7
Air gap, mm	1.5	1.5	1.5
Magnet axial length, mm	5	5	5
Magnet remanence, T	1.22	1.22	1.22
Number of turns per coil	25	50	50

The derivation of the sizing equation follows a similar form to the sizing equation as in [15-18]:

$$P = \frac{\pi^2 n p l_m \left(R_o^2 - R_i^2\right) R_i}{60\left(l_m + g'\right)} l_{bar} J K_f \alpha_s B_r \left(1 - \frac{\alpha_s l_m B_r}{\left(l_m + g'\right) B_s}\right) \quad (1)$$

where P is the output power, n is machine speed, R_o, R_i are stator outer and inner radius respectively, l_{bar} is winding axial length, J is winding current density, K_f is winding fill factor, l_m is magnet thickness and g' is effective air gap length, B_r and B_s are magnet residual flux density and maximum no load stator core flux density. The stator, magnet outer to inner diameter ratio is chosen as 0.58 for maximum specific torque, in equation (1). The main design parameters are summarized in Table I.

Cogging torque is one of the main contributors to the torque ripple in PM motors, which is caused by the interactions between PMs and stator teeth. Beside pole and slot combination, pole arc has significant effect on cogging torque. In this research cogging torque of three machines are set at their minimum for different configuration. The optimum ratios of pole arc to pole pitch for minimizing cogging torque for a given slot and pole number is [18-21]:

$$\alpha_p = \frac{N - k_1}{N} + k_2 \quad , \qquad k_1 = 1, 2, \ldots, N-1 \qquad (2)$$

where $N=N_c/2p$, N_c is the least common multiple between pole number and slot number, and k_2 is a constant that ranges from 0.01 to 0.03 depending on air-gap length [22-26]. Equation (2) is for a regular machine with equal tooth widths. Optimum pole arc to pole pitch ratios of a 12-slot/10-pole machine with unequal tooth widths is equal to the optimum pole arc to pole pitch ratios of a 6-slot/10-pole machine with equal tooth widths. Hence, the optimum ratios of pole arc to pole pitch for minimizing cogging torque is shown in Table II. The common pole arc to pole pitch ratio of 0.7 was chosen for this study.

TABLE II. OPTIMUM POLE ARC TO POLE PITCH RATIOS

12-slot/10-pole	0.19, 0.36, 0.53, 0.7, 0.86
12-slot/10-pole with unequal tooth widths	0.36, 0.7

Parallel stator slot-openings are used so that high filling factor can be achieved. When parallel slot-openings are employed, the ratio of the slot-opening width to the slot-pitch is a function of radius. In the case of machines A and B, the tooth widths at every radius (r) can be obtained as:

$$w = r\left(2\pi/N_s - 2\sin^{-1}\left(ds/2r\right)\right) \tag{3}$$

while in the case of machines with unequal tooth widths as machine C, the tooth widths at every radius (r) can be obtained as:

$$w_c = r\left(\pi/p - 2\sin^{-1}\left(ds/2r\right)\right) \tag{4}$$

$$w_n = r\left(4\pi/N_s - \pi/p - 2\sin^{-1}\left(ds/2r\right)\right) \tag{5}$$

where w_c is the width of teeth that carries a coil, w_n is the width of teeth that does not carry a coil, P is the number of pole pairs, N_s is the number of slot, and ds is the parallel slot-opening.

There are different ways to realize a motor with concentrated windings. It is assumed that the design is performed for three-phase motors with balanced windings which have two coils sides in each slot. The angles of the kth coil for the double-layer concentrated windings are defined as:

$$\theta_c(k) = (k-1)\frac{p}{N_s}180^\circ E \quad \text{for } k = 1,\ 2,\ \ldots,\ N_s \tag{6}$$

while for the single-layer winding as:

$$\theta_c(k) = (k-1)\frac{p}{N_s}360^\circ E \quad \text{for } k = 1,\ 2,\ \ldots,\ N_s/2 \tag{7}$$

with respect to (6) and (7), in a double-layer 12-slot/10-pole machine the 3-phase winding arrangement is AA′C′CBB′A′ACC′B′B; and for a single-layer 12-slot/10-pole machine, either for equal or unequal tooth widths, it is AC′BA′CB′.

The winding factors K_{wn} can be achieved as:

TABLE III. WINDING FACTOR

Motor Type	Harmonic order			
	n = 1	n = 3	n = 5	n = 7
Motor A	0.933	0.5	0.067	0.067
Motor B	0.966	-0.707	0.259	0.259
Motor C	1	1	1	1

$$k_{wn} = \frac{1}{N_{cph}}\sum_{k=1}^{N_{cph}} e^{-jn\theta_c(k)} \tag{8}$$

where N_{cph} represents number of coils per phase.

III. SIMULATION RESULTS

The finite-element method allows a precise analysis of magnetic devices taking into account geometric details and magnetic nonlinearity. As axial-flux PM machines are inherently 3-D machines, 3-D finite-element model was developed to simulate the performance of the machines. Phase back-EMF, winding inductance, cogging torque, and output torque are obtained for three machines with precise 3-D finite-element simulation.

Table III shows the winding factors for the fundamental and harmonics of the motors. It can be seen that motor C, having single-layer windings with unequal tooth widths has highest fundamental winding factor. This could result in higher flux linkage and consequently higher torque compared to other two motors.

Torque quality of AFPM machines, which is directly related to the torque ripple components, is of high importance. Torque ripple, which is the torque pulsation caused by the periodic components in the instantaneous torque of the machine, could result in vibration, noise, and even failure. The torque ripple of PM BLDC machine constitutes two different components, back-EMF related torque ripple, and cogging torque which is unaffected by the load. The contribution of these components in toque ripple is investigated in following.

A. Phase back-EMF and Line back-EMF

Phase back-EMF is computed by the no-load change rate of flux linkage through the corresponding coils. Phase-back-EMF and line back-EMF waveforms of the three motors are obtained by using 3-D finite-element model and are shown in Figures 2 and 3; respectively. It is seen that machines with single layer windings has more trapezoidal phase back-EMF waveforms. Also unequal tooth widths will increase the flat top area and hence machine C has the most trapezoidal phase back-EMF waveform. As in brushless-dc operation, only two phases conduct at each time, line back-EMF waveform will define the average electromagnetic torque and also back-EMF related torque ripple. It is seen that motors B and C have a high line back-EMF value, while motor A with double-layer windings has the lowest value. Also it is seen from Figure 3 that machine B has the least flat top area. So machine B with single layer winding and equal tooth widths will have higher back-EMF related torque ripple.

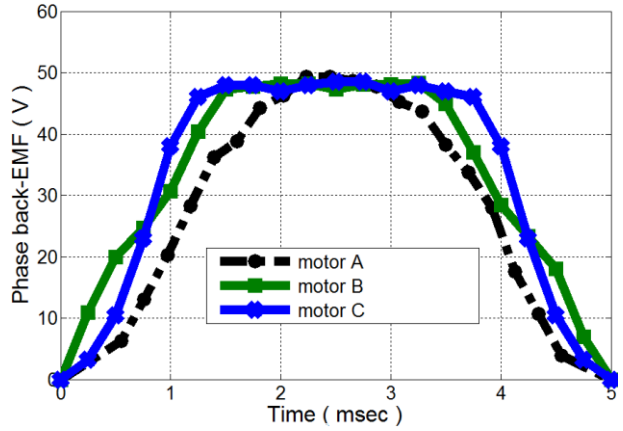

Figure 2. Phase back-EMF waveforms by 3-D finite-element

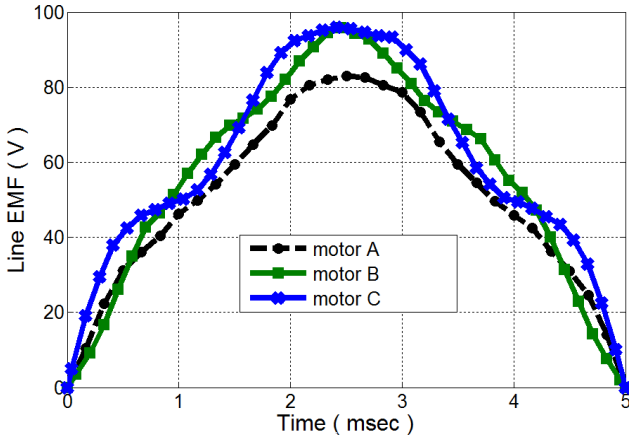

Figure 3. Line EMF waveforms by 3-D finite-element

B. *Winding Inductances and Cogging Torque*

Table IV shows self and mutual inductances of the three machines obtained by 3-D finite-element model. It is seen that machines B and C have higher self-inductance which can limit short circuit current better than machine A. Also machines B and C have lower mutual-inductance which will isolate phases from each other more effectively compared to motor A. So motors B and C which have single layer windings provide higher fault tolerance capability.

The number of cogging torque periods per rotor revolution is equal to the LCM (least common multiple) of poles number and slots number. Higher cogging torque frequency leads to lower magnitude. It is clear that machines A and B have the same cogging torque as winding layer numbers do not influence cogging torque. Also the cogging torque waveform of the 12-slot/10-pole machine C with unequal tooth widths is similar to that of a 6-slot/10-pole machine with equal tooth widths. It should be mentioned that for computing cogging torque waveforms having extremely low amplitude, mesh density in the finite element analysis has to be significantly high. Cogging torque waveforms of the three axial-flux PM machines are obtained using 3-D finite-element analysis as shown in Fig. 4. In machines A and B, the number of cogging

TABLE IV. SELF AND MUTUAL INDUCTANCES

Motor Type	Self-inductance (mH)	Mutual inductance (mH)
Motor A	1.21	0.106
Motor B	1.95	-0.026
Motor C	2.15	-0.037

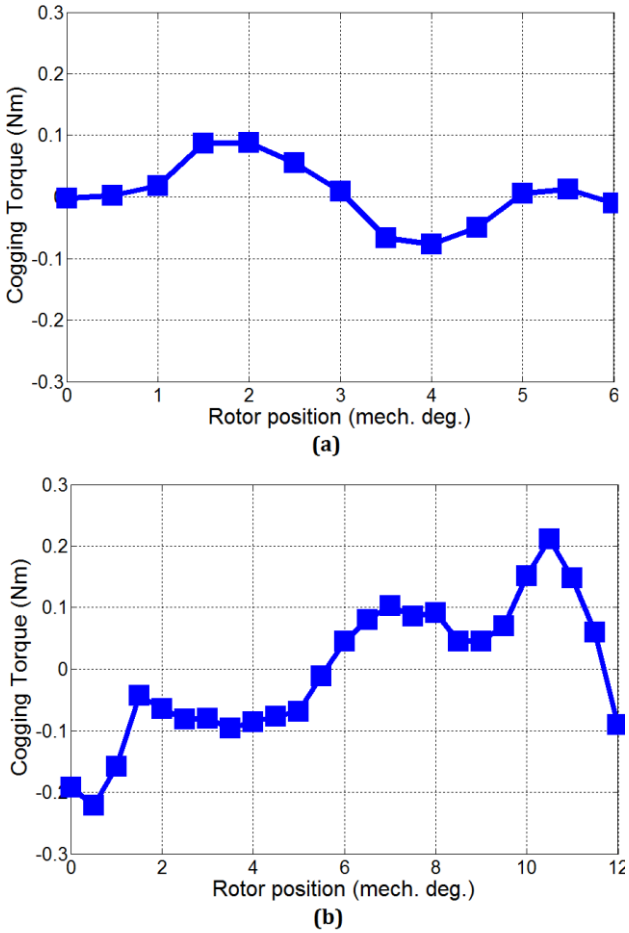

Figure 4. Cogging torque waveforms for (a) motors A and B, (b) motor C

torque periods per revolution is 60, while it is 30 for machine C. As can be seen in Figure 4, higher cogging torque frequency results in lower level of the cogging torque. The peak to peak cogging torque of all three motors is extremely low, about 0.2 Nm for machines A and B with equal tooth widths, and about 0.4 Nm for machine C with unequal tooth widths.

C. *Output Torque*

The instantaneous electromagnetic torque of the machine can be calculated from:

$$T = \frac{1}{w_r}\left(e_a i_a + e_b i_b + e_c i_c\right) \tag{8}$$

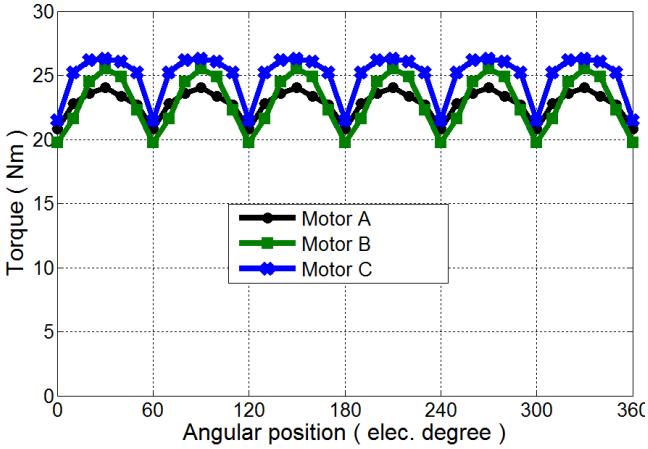

Figure 5. 3-D finite-element output torque waveforms

TABLE V. MOTOR PERFORMANCES

Type	T_{max} (Nm)	T_{min} (Nm)	T_{ave} (Nm)	T_{ripple} (%)
Motor A	24.05	20.8	22.60	14.37
Motor B	25.51	19.73	22.84	25.31
Motor C	26.27	21.49	24.56	19.46

where e_a, e_b, e_c, i_a, i_b, and i_c are back-EMFs and currents in phases A, B, and C, respectively. Also w_r is the rotor speed (rad/s). Torque waveform has dominant information about motor performance including torque average and torque ripple, and the motor choice for different applications can be based on it. All of the three machines considered in this research are supplied with 120˚ rectangular phase current waveforms (brushless-dc operation) with 34-A amplitude. The torque was obtained by using 3-D finite-element analysis as shown in Figure 5. Maximum torque, minimum torque, average torque and torque ripple of the motors are given in Table V. It is seen that motor C with single layer windings and unequal tooth widths has highest torque value with medium torque ripple which makes it appropriate for applications requiring high torque-density. Also, motor A with double layer windings has the least torque ripple which makes it a good candidate for applications where low noise and vibration is important. Motor B with single layer windings and equal tooth widths has the highest torque ripple.

IV. CONCLUSION

Analysis and comparison of axial-flux PM BLDC machines by 3-D finite-element analysis was presented in this paper. The comparison is done for three 10-pole machines with the same dimensions, magnetic and electric loading. It is shown that although all three axial-flux PM machines have good fault tolerance capability, but axial-flux PM machines with single layer windings can better fulfill fault tolerance capability. Also all machines, having similar slot number and pole number and chosen pole arc to pole pitch ratio, produced low cogging torque. Axial-flux PM machines with single layer windings and unequal tooth widths have the highest torque average, while axial-flux PM machines with double-layer windings had the lowest torque ripples.

REFERENCES

[1] G. De Donato, F. G. Capponi and F. Caricchi, “On the use of magnetic wedges in axial flux permanent magnet machines”, IEEE Trans Ind Electron, vol 60, pp. 4831-4840, 2013.

[2] R. Di Stefano and F. Marignetti, “Electromagnetic analysis of axial-flux permanent magnet synchronous machines with fractional windings with experimental validation” IEEE Trans Ind Electron, vol 59, pp. 2573-2582, 2012.

[3] K. Sitapati and R. Krishnan, “Performance comparisons of radial and axial field permanent magnet brushless machines”, IEEE Trans Ind Appl, vol 37, pp. 1219–1226, 2001.

[4] S. M. Hosseini, M. Agha-Mirsalim and M. Mirzaei, “Design, prototyping, and analysis of low cost axial-flux coreless permanent-magnet generator”, IEEE Trans Magn, vol 44, pp. 75-80, 2008.

[5] A. Di Gerlando, G. Foglia, R. Perini and M. Iacchetti, “Axial flux PM machines with concentrated armature windings: Design analysis and test validation of wind energy generators”, IEEE Trans Ind Electron, vol. 58, pp. 3759-3805, 2011.

[6] E. Bostanci, Z. Neuschl, R. Plikat and B. Ponick, “No-Load Performance Analysis of Brushless DC Machines with Axially Displaceable Rotor”, IEEE Trans Ind Electron, vol. 61, pp. 1692-1699, 2014.

[7] N. A. Rahim, H. W. Ping and M. Tadjuddin, “Design of axial flux permanent magnet brushless DC motor for direct drive of electric vehicle”, In: IEEE Power Engineering Society General Meeting, Tampa, USA, pp. 1-6, June 2007.

[8] W. Jiabin, Y. Xibo and K. Atallah, “Design Optimization of a Surface-Mounted Permanent-Magnet Motor With Concentrated Windings for Electric Vehicle Applications”, IEEE Tran Vehicular Technology, vol. 62, pp. 1053-1064, 2013.

[9] S. S. Nair, Sh. Nalakath and S. J. Dhinagar, “Design and analysis of axial flux permanent magnet BLDC motor for automotive applications’, In: IEEE International Electrical Machines and Drive Conference, Niagara Falls, Canada, pp. 1615-1618, May 2011.

[10] T. J. Woolmer and M. D. McCulloch, “Analysis of the yokeless and segmented armature machine”, In: IEEE Int Electric Machines & Drives Con, Anatlya, Turkey, pp. 704-708, 2007.

[11] W.Fei and P.C.K.Luk, “Cogging Torque Reduction Techniques for Axial-Flux Surface-Mounted Permanent-Magnet Segmented-Armature-Torus Machines” pp. 485-490, 2008.

[12] S. Jafarishiadeh, M. Ardebili, A. Nazari Marashi, “Investigation of pole and slot numbers in axial-flux pm bldc motors with single-layer windings for electric vehicles,” 24th *Iranian Conference on Electrical Engineering (ICEE)*, pp. 1444-1448, 2016.

[13] S. M. Jafari-Shiadeh and M. Ardebili, “Analysis and comparison of axial-flux permanent-magnet brushless-DC machines with fractional-slot concentrated-windings”, Proc. 4th Annu. Int. Power Electron., Drive Syst., Technol. Conf., pp. 72-77, 2013.

[14] Khazaei, P., S. M. Modares, M. Dabbaghjamanesh, M. Almousa, and A. Moeini. "A high efficiency DC/DC boost converter for photovoltaic applications." International Journal of Soft Computing and Engineering (IJSCE) 6, no. 2 (2016): 2231-2307.

[15] S. Jafari-Shiadeh, M. Ardebili, and P. Moamaei, “Three-dimensional finite-element-model investigation of axial-flux PM BLDC machines with similar pole and slot combination for electric vehicles”, *Proceedings of Power and Energy Conference*, Illinois, pp. 1–4, 2015.

[16] Z. Q. Zhu and D. Howe, “Improved Analytical Model for Predicting the Magnet Field Distribution in Brushless Permanent-Magnet Machines,” IEEE Tran on Magn, vol. 38, pp. 229-238, 2002.

[17] A. M. Bozorgi, M. Monfared, and H. R. Mashhadi, “Two simple overmodulation algorithms for space modulated three-phase to three-phase matrix converter,” *IET Power Electron*., vol. 7, no. 7, pp. 1915–1924, Jul. 2014

[18] I. Mazhari, H. Jafarian, B. Parkhideh, S. Trivedi, and S. Bhowmik, “Locking Frequency Band Detection Method for Grid-tied PV Inverter Islanding Protection,” *IEEE Energy Conversion Congress and Exposition (*ECCE), Montreal, QC, pp. 1976-1981, 2015.

[19] Khazaei, Peyman, Morteza Dabbaghjamanesh, Ali Kalantarzadeh, and Hasan Mousavi. "Applying the modified TLBO algorithm to solve the unit commitment problem." In World Automation Congress (WAC), 2016, pp. 1-6. IEEE, 2016.

[20] A. Bozorgi, M. Farasat, and S. Jafarishiadeh, "Improved model predictive current control of permanent magnet synchronous machines with fuzzy based duty cycle control," *2016 IEEE Energy Conversion Congress and Exposition (ECCE)*, Milwaukee, WI, USA, 2016, pp. 1-6.

[21] M. Khodabandeh, M. R. Zolghadri, M. Shahbazi and N. Noroozi, "T-type direct AC/AC converter structure," in IET Power Electronics, vol. 9, no. 7, pp. 1426-1436, 6 8 2016.

[22] M. Dabbaghjamanesh, A. Moeini, M. Ashkaboosi, P. Khazaei, and K. Mirzapalangi, "High performance control of grid connected cascaded H-bridge active rectifier based on type II-fuzzy logic controller with low frequency modulation technique," *International Journal of Electrical and Computer Engineering*, vol. 6, no. 2, pp. 484–494, Apr. 2016.

[23] A. M. Bozorgi, V. Fereshtehpoor, M. Monfared, N. Namjoo, "Controller Design Using Ant Colony Algorithm for a Non-inverting Buck–Boost Chopper Based on a Detailed Average Model", *Electric Power Components and Systems*, vol. 43, no. 2. 2015.

[24] A. M. Bozorgi, M. Monfared, and H. R. Mashhadi, "Optimum switching pattern of matrix converter space vector modulation," *in Computer and Knowledge Engineering (ICCKE)*, 2012 2nd International eConference on , 18-19 Oct. 2012 2012, pp. 89–93.

[25] A. M. Bozorgi, M. Sanatkar Chayjani, R. Mohammad Nejad, and M. Monfared, "Improved grid voltage sensorless control strategy for railway power conditioners," *Power Electronics, IET*, vol. 8, pp. 2454-2461, 2015.

[26] Ashkaboosi, Maryam, Seyed Mehdi Nourani, Peyman Khazaei, Morteza Dabbaghjamanesh, and Amirhossein Moeini. "An optimization technique based on profit of investment and market clearing in wind power systems." American Journal of Electrical and Electronic Engineering 4, no. 3 (2016): 85-91.